

SEEING THROUGH THE DARKNESS: VISUALIZING LOW FREQUENCY BEHAVIOR IN SMALL ROOMS

AJ Hill
MOJ Hawksford

Audio Research Laboratory, University of Essex, Colchester, UK
Audio Research Laboratory, University of Essex, Colchester, UK

1 INTRODUCTION

Low-frequency acoustical behavior in small-sized listening rooms can be a significant source of widely varying listening experiences due to the occurrence of multiple reflections from various boundaries which in the steady state lead to standing waves. A great deal of research has focused on both actively and passively dealing with this problem including passive/active absorption, single/multiple point equalization and subwoofer configuration (location, polar pattern, time alignment)¹⁻⁷. These techniques, either alone or together, can provide significant improvement in low-frequency behavior giving listeners much similar experiences, regardless of location within the listening space.

The ability to visualize and analyze these various control techniques in the virtual world can be extremely helpful in determining the combination of low-frequency control methods to utilize in a room in the search for the best possible low-frequency response. This paper describes a computational toolbox that provides visualization/analysis specifically aimed at low-frequency behavior. The toolbox operates under the Finite-Difference Time-Domain (FDTD) simulation paradigm which can provide accurate low-frequency data and is also highly flexible in terms of room shape, subwoofer location(s) and virtual listening locations.

A brief background of low-frequency room acoustics will be presented as well as an overview of the FDTD simulation method utilized for this program. Key features of the toolbox will be highlighted including steady state visualizations, theoretical room mode validation, single versus multiple subwoofer system comparisons, diffraction analysis and acoustical behavior of a network of interconnected rooms.

2 SMALL ROOM ACOUSTICS

The root of many acoustical problems in rooms is resonant modes. These modes are the result of the formation of standing waves where the resonant frequencies relate to the dimensions of a room and are present in all acoustical spaces. The standing waves are formed when the dimensions of the room are integer multiples of the half-wavelength corresponding to a given frequency⁸. In specific frequency bands this can result in significant differences in sound level as a listener moves about the room. Prediction of these discrete room modes can be determined for rectangular spaces using the equation⁸

$$f = \frac{c}{2} \sqrt{\left(\frac{l}{L_x}\right)^2 + \left(\frac{m}{L_y}\right)^2 + \left(\frac{n}{L_z}\right)^2} \quad \text{for } l, m, n = 0, 1, 2 \dots \quad [1]$$

where: f = modal frequency (Hz)
 c = speed of sound (m/s)
 L_x = length of room (m)
 L_y = width of room (m)
 L_z = height of room (m)

These calculated room modes occur across the entire frequency spectrum, but only pose acoustical problems below a certain crossover frequency referred to as the Schroeder frequency, f_c . Below this frequency, the spatial patterns of the room modes are sufficiently delineated to be noticeable as a listener moves about the room. Above the Schroeder frequency, the field is considered diffuse, where the modal patterns, while still present, significantly overlap making it impossible to notice distinct modes.

$$f_c = 2000 \sqrt{\frac{T_{60}}{V}} \quad [2]$$

where: f_c = Schroeder frequency (Hz)
 T_{60} = room reverberation time (s)
 V = room volume (m^3)

This equation, which first appeared in Schroeder's 1954 paper⁹, initially had a multiplier constant of 4000 that was changed to 2000 in Schroeder's 1996 paper¹⁰. Below the Schroeder frequency, it is important to have a method to quantify the variation in response across a room. Two common metrics used for this purpose are called magnitude deviation and spatial variance. Magnitude deviation is a measure of how much the frequency response at a single location deviates from flat across a given frequency band. This value is calculated for each listening location in a room and averaged to give a single metric expressed in dB (Equation 3)⁶. The closer the magnitude deviation is to 0 dB, the closer the room response is to a "flat" response.

$$MD = \sqrt{\frac{1}{n_f - 1} \sum_{i=f_{low}}^{f_{high}} (x_i - \bar{x})^2} \quad [3]$$

where: MD = magnitude deviation (dB)
 n_f = number of frequency bins
 f_{high} = upper frequency limit (Hz)
 f_{low} = lower frequency limit (Hz)
 x_i = sound pressure at frequency bin, i
 \bar{x} = average sound pressure at that frequency or listening location

Spatial variation, on the other hand, is a measure of how much variation there is from point to point in a room at a single frequency. This is taken for each frequency bin contained in a specified band and averaged together to give a single metric (Equation 4)⁶. Like magnitude deviation, this is measured in dB and the closer the spatial variance is to 0 dB, the less noticeable the modal behavior of the room.

$$SV = \frac{1}{n_f} \sum_{i=f_{low}}^{f_{high}} \sqrt{\frac{1}{n_p - 1} \sum_{p=1}^{n_p} (x_{p,i} - \bar{x})^2} \quad [4]$$

where: SV = spatial variance (dB)
 n_p = number of listening locations
 $x_{p,i}$ = sound pressure at frequency bin, i , and listening location, p

Using magnitude deviation and spatial variance in tandem allows adjustments to be made to a room/playback system to minimize both deviations across the room and across the frequency spectrum.

3 FDTD SIMULATION

The finite-difference time-domain (FDTD) simulation method has existed since the 1960's where it has been used extensively in electromagnetics research. FDTD has been steadily gaining popularity in acoustics over the past couple decades due to a number of key advantages it has over other acoustics modeling techniques. FDTD operates using a group of fixed grids that operate in a leap-frog scheme as depicted in Figure 1¹¹.

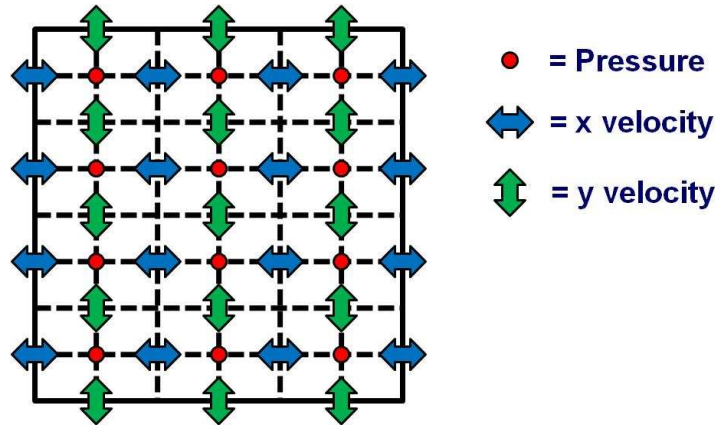


Figure 1: Grid structure of FDTD simulation

The simulation begins with a predefined sound pressure level at the source location(s). This pressure value is then used to update the surrounding particle velocity points. These points, in turn, are used to calculate the surrounding pressure point, including those at the source location(s). This computation progresses until the simulation reaches its conclusion. As illustration of the technique, some of the equations incorporated into a 3D FDTD simulation are shown below which have been adapted from 2D equations¹².

$$u^x_{x+\frac{dx}{2},y,z} \left(t + \frac{dt}{2} \right) = u^x_{x+\frac{dx}{2},y,z} \left(t - \frac{dt}{2} \right) - \frac{dt}{\rho dx} [p_{x+dx,y,z}(t) - p_{x,y,z}(t)] \quad [5]$$

$$u^y_{x,y+\frac{dy}{2},z} \left(t + \frac{dt}{2} \right) = u^y_{x,y+\frac{dy}{2},z} \left(t - \frac{dt}{2} \right) - \frac{dt}{\rho dy} [p_{x,y+dy,z}(t) - p_{x,y,z}(t)] \quad [6]$$

$$u^z_{x,y,z+\frac{dz}{2}} \left(t + \frac{dt}{2} \right) = u^z_{x,y,z+\frac{dz}{2}} \left(t - \frac{dt}{2} \right) - \frac{dt}{\rho dz} [p_{x,y,z+dz}(t) - p_{x,y,z}(t)] \quad [7]$$

$$p_{x,y,z}(t + dt) = p_{x,y,z}(t) - \frac{c^2 \rho dt}{dx} \left[u^x_{x+\frac{dx}{2},y,z} \left(t + \frac{dt}{2} \right) - u^x_{x-\frac{dx}{2},y,z} \left(t + \frac{dt}{2} \right) \right] \\ - \frac{c^2 \rho dt}{dy} \left[u^y_{x,y+\frac{dy}{2},z} \left(t + \frac{dt}{2} \right) - u^y_{x,y-\frac{dy}{2},z} \left(t + \frac{dt}{2} \right) \right] \\ - \frac{c^2 \rho dt}{dz} \left[u^z_{x,y,z+\frac{dz}{2}} \left(t + \frac{dt}{2} \right) - u^z_{x,y,z-\frac{dz}{2}} \left(t + \frac{dt}{2} \right) \right] \quad [8]$$

where: u^x = particle velocity in the x-direction (m/s)
 u^y = particle velocity in the y-direction (m/s)
 u^z = particle velocity in the z-direction (m/s)
 $p_{x,y,z}$ = pressure at point (x,y,z) (Pa)
 t = time (s)

- dt = time step (s)
- dx = grid spacing in the x-direction (m)
- dy = grid spacing in the y-direction (m)
- dz = grid spacing in the z-direction (m)
- ρ = air density (kg/m³)
- c = speed of sound in air (m/s)

Care must be taken at boundary conditions since pressure points do not exist beyond the walls of the room (for simplified simulations, at least). Special equations must be put to use to address this problem which uses a wall's absorption coefficient to determine the reflection back into the room¹².

$$u_{L_x,y,z}^x \left(t + \frac{dt}{2} \right) = \frac{R_x - Z}{R_x + Z} u_{L_x,y,z}^x \left(t - \frac{dt}{2} \right) + \frac{2}{R_x + Z} p_{x,y,z}(t) \tag{9}$$

$$Z = \rho c \frac{1 + \sqrt{1 - \alpha}}{1 - \sqrt{1 - \alpha}} \tag{10}$$

- where: L_x = length of the room (m)
- L_y = width of the room (m)
- L_z = height of the room (m)
- R_x = $\frac{\rho dx}{dt}$
- R_y = $\frac{\rho dy}{dt}$
- R_z = $\frac{\rho dz}{dt}$
- Z = characteristic wall impedance
- α = wall absorption coefficient

Unlike image source or ray tracing techniques that operate based on the sound propagation paths from a source to a listening point in a room, FDTD focuses on the interaction of adjacent points in the room so a user can make the grid as fine as needed. This allows for very precise low frequency modeling where the other techniques tend to lose accuracy as frequency wavelengths approach and surpass the dimensions of a room.

A second advantage to FDTD is the ease of simulation setup. Thanks again to the grid structure of FDTD, any point within the grid system can be designated as a source or a listening point. Also, room boundaries can be readily defined by adjusting the grids from rectangular to non-rectangular dimensions with the help of grid masks¹¹, for example see Figure 2.

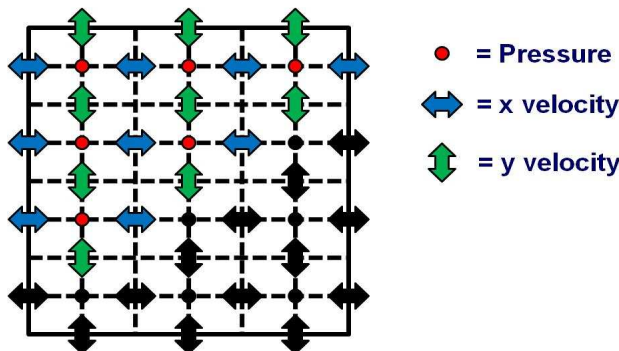


Figure 2: Adjusted grid layout to allow for non-rectangular spaces

The innate flexibility within the simulation setup allows modeling of virtually any imaginable room/playback system. Also, straightforward grid manipulation allows the insertion of obstacles into the acoustic path which can be crucial in order to obtain the most realistic simulation results.

4 SIMULATION TOOLBOX FEATURES

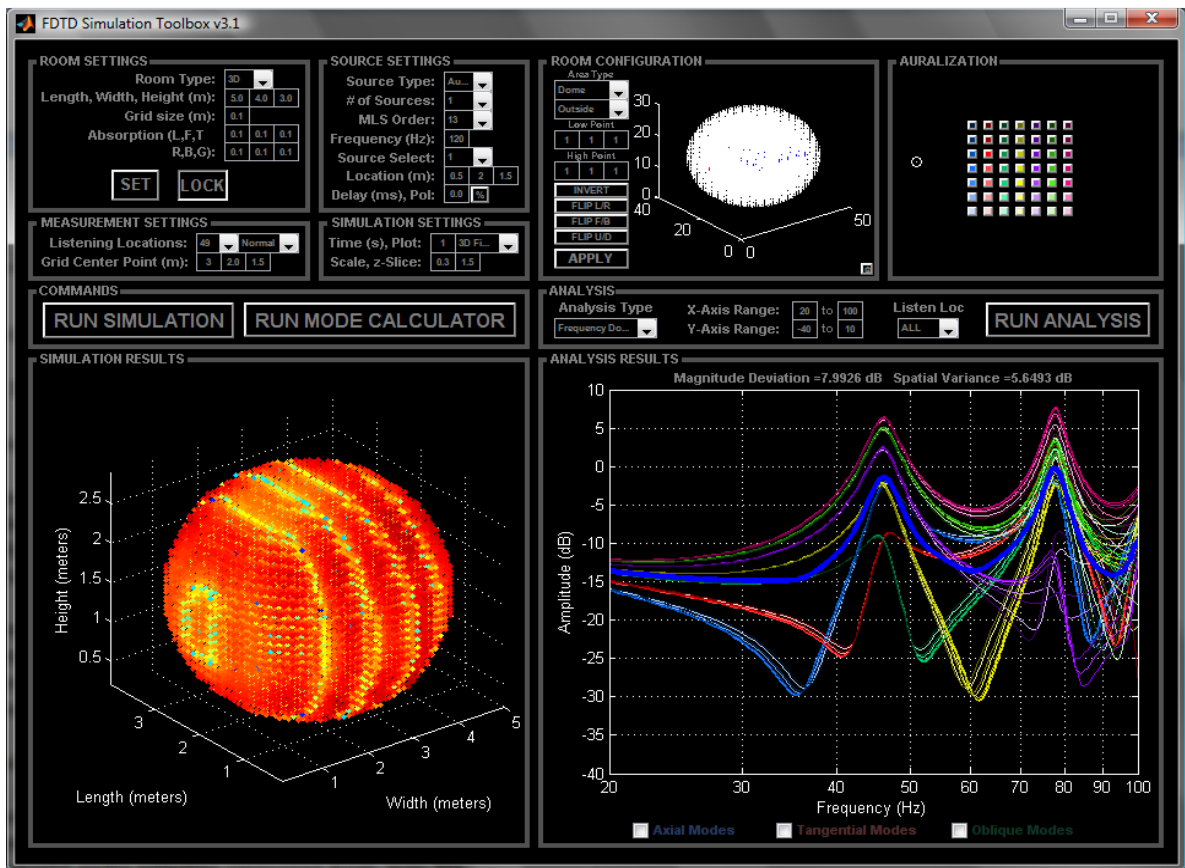


Figure 3: FDTD simulation toolbox GUI layout in MATLAB

The FDTD simulation toolbox was written to give a wide variety of simulation/analysis options and flexibility while also maintaining ease of use. The toolbox has been laid out in an easy to use GUI in Matlab. All simulation setup operations are performed in the upper half of the window while simulation and analysis visualization are displayed in the lower half.

A user would first initialize all room variables including the dimensions, simulation grid size and wall absorption. Once entered, a graphical display of the pressure grid is displayed in the room configuration window, where by default the pressure grid is set to zero. Next, the user can modify this pressure grid by selecting nodes in the grid and removing (or adding) them to be inside the room as shown in Figure 4. This procedure allows for both non-rectangular spaces as well as for obstacles to be placed in the room.

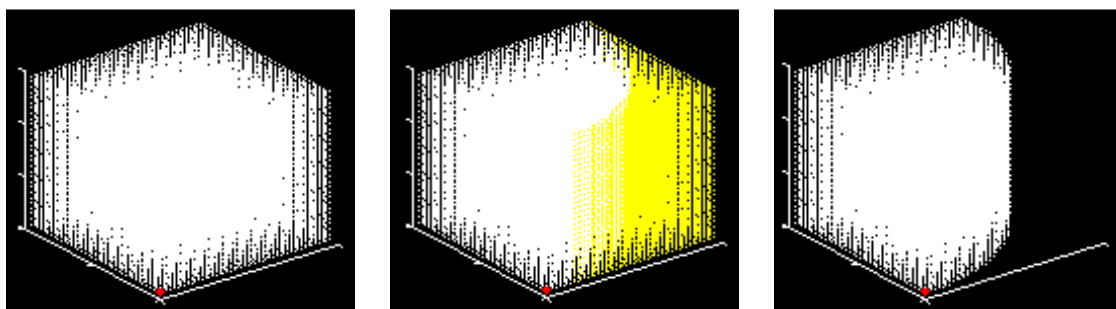


Figure 4: Defining a non-rectangular space in the “Room Configuration” section of the toolbox

Next, a user inputs all the source information including number of sources, location, delay, polarity and source signal type. Once the room and source(s) have been set, a listening point or grid node must be defined and placed in the room. All adjustments to the grid placement and size are reflected in the “Room Configuration” section of the toolbox. Finally, the type of simulation output is selected. This can be an animation of the sound propagation in the room (2D or 3D), an SPL plot of the room at the conclusion of the simulation or, no simulation plot, best when using the toolbox primarily for its analysis section as illustrated in Figure 5.

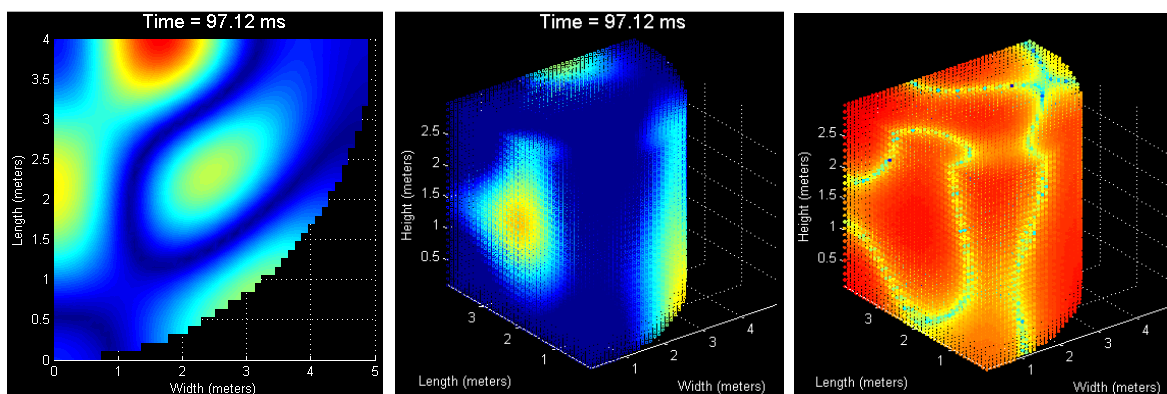


Figure 5: 2D (left) & 3D (center) animation snapshot and final SPL plot (right) of a 120 Hz source

Once the simulation is complete, the analysis section can be used to explore the data collected at each virtual listening location. The user can perform a number of time/frequency analysis operations including SPL vs. time, SPL vs. frequency and spectrogram plots, see Figure 6 & 7. The frequency analysis options allow for an overlapping plot of expected axial, tangential and oblique frequencies calculated using Equation 1 and illustrated in Figure 7. The frequency analysis options can also display both the magnitude deviation and spatial variance values calculated from Equations 3 and 4, if the listening grid contains more than one point.

In addition to the analysis plots and metrics, a simple auralization function is available if the source signal used is a real-world audio signal (.wav file). If so, a number of colored boxes will appear in the auralization section which correspond to the points in the listening grid. A user simply clicks on any button to hear what was simulated at that point. The function currently operates by splitting the signal into low and high frequency bands via a crossover filter and then sending the low frequency component through the FDTD simulation. The high frequency signal is then appropriately delayed and recombined with the processed low-frequency component to achieve a broad-band signal for audition.

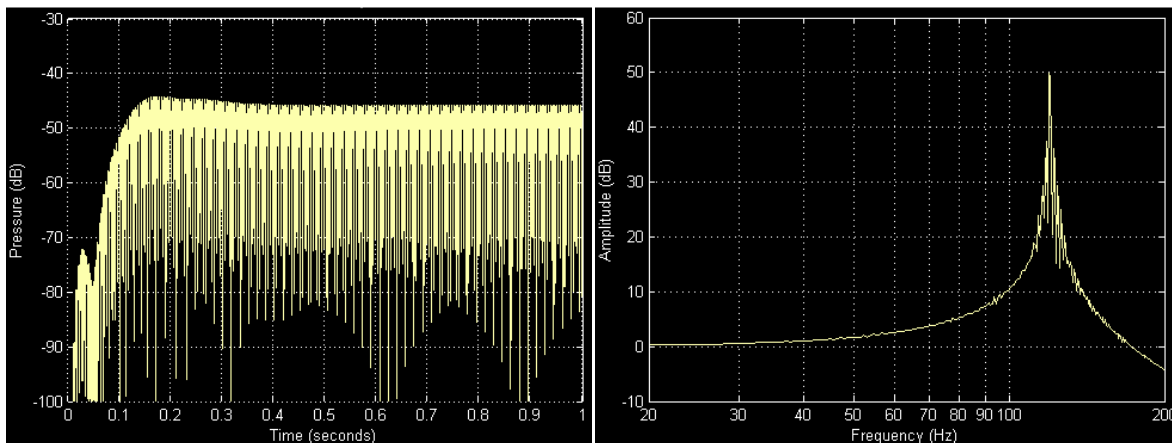


Figure 6: Time vs. SPL (left) and frequency vs. SPL (right) plots for a 120 Hz source at a single point in the listening grid of the simulation from Figure 5

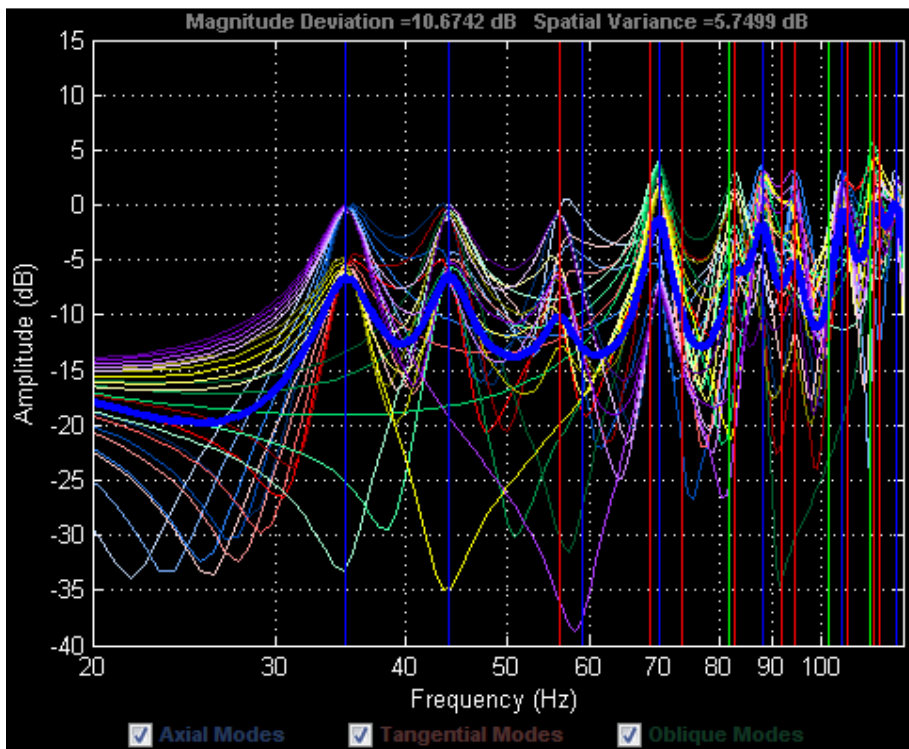


Figure 7a: SPL vs. frequency plot for an MLS source signal in a rectangular 5 m x 4 m x 3 m room with axial, tangential and oblique modes overlaid

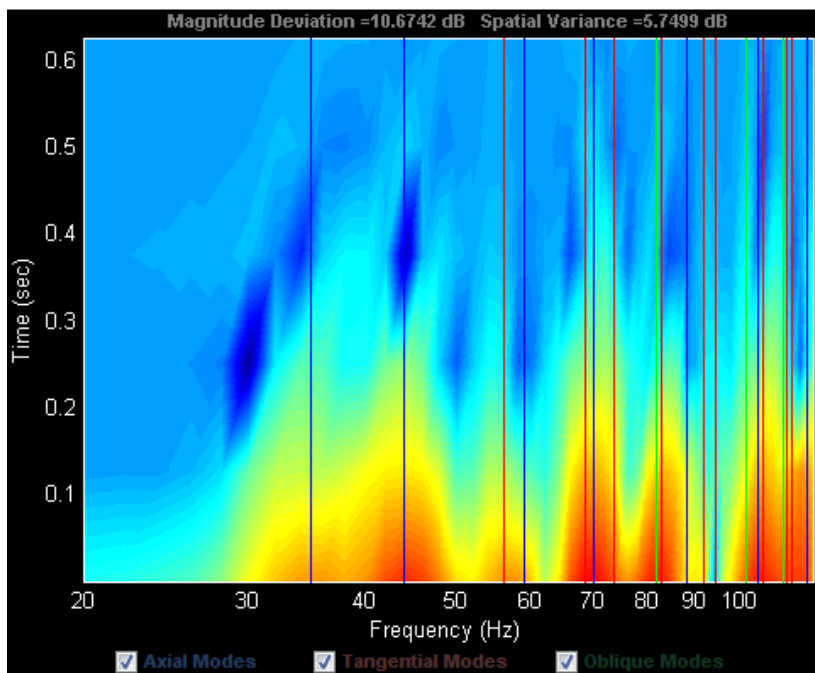


Figure 7b: Spectrogram plot for an MLS source signal in a rectangular 5 m x 4 m x 3 m room with axial, tangential and oblique modes overlaid

5 SIMULATION EXAMPLES

The FDTD simulation toolbox can be used to perform a number of different types of acoustic simulations. One basic test that can be performed is the analysis of the steady state sound pressure distribution for a single modal frequency. For example, if a rectangular room was simulated with dimensions 5 m x 4 m x 3 m, Equation 1 would predict an axial mode at 68.6 Hz. Using a function built into the toolbox called the “room mode calculator”, a three dimensional plot can be generated which predicts the locations of the nodes and antinodes for the steady state of the specific modal frequency. This can be compared to the final SPL plot from the simulation to validate the results (Figure 8).

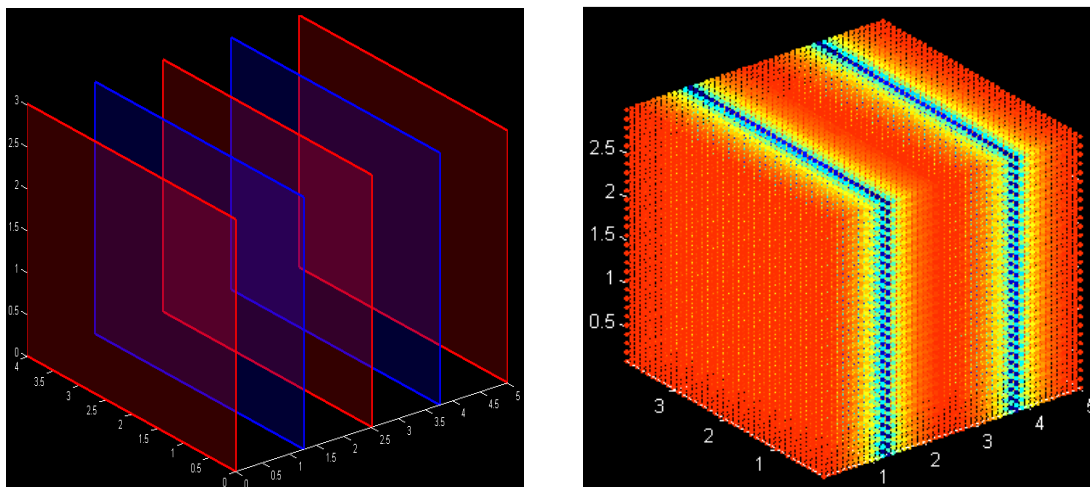


Figure 8: Calculated (left) and simulated (right) distribution of an axial mode at 68.6 Hz in a 5 m x 4 m x 3 m room (blue = nodes, red = antinodes)

The same can be done for tangential and oblique modes located at 109.8 and 158.5 Hz, respectively, where the results are displayed in Figures 9 and 10.

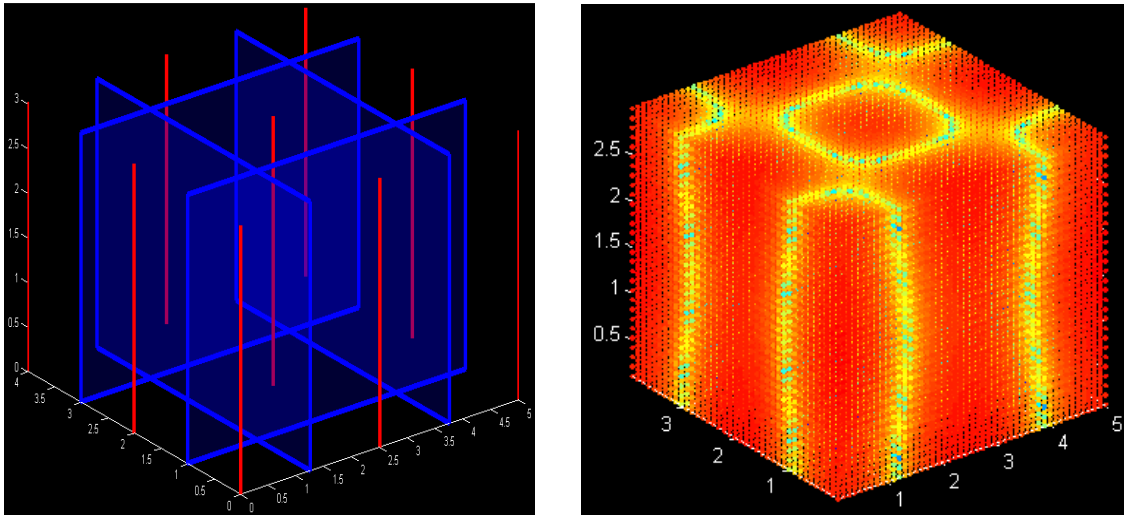


Figure 9: Calculated (left) and simulated (right) distribution of a tangential mode at 109.8 Hz in a 5 m x 4 m x 3 m room (blue = nodes, red = antinodes)

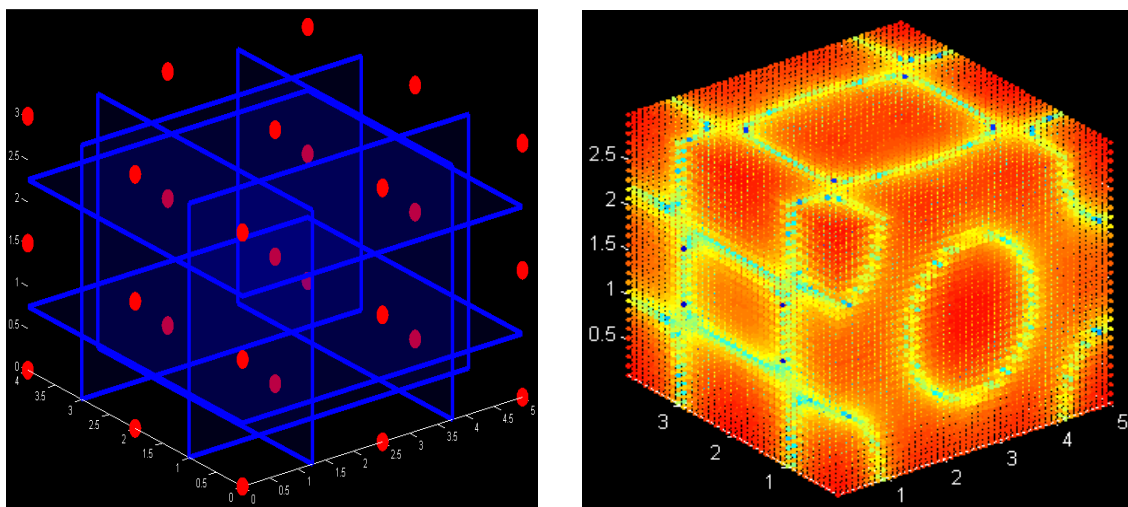


Figure 10: Calculated (left) and simulated (right) distribution of an oblique mode at 158.5 Hz in a 5 m x 4 m x 3 m room (blue = nodes, red = antinodes)

In addition to these steady state visualizations, the animation function in the toolbox allows a user to actually view the process leading up to and including the steady state of a single sinusoidal frequency in a room, where an illustration is shown in Figure 11.

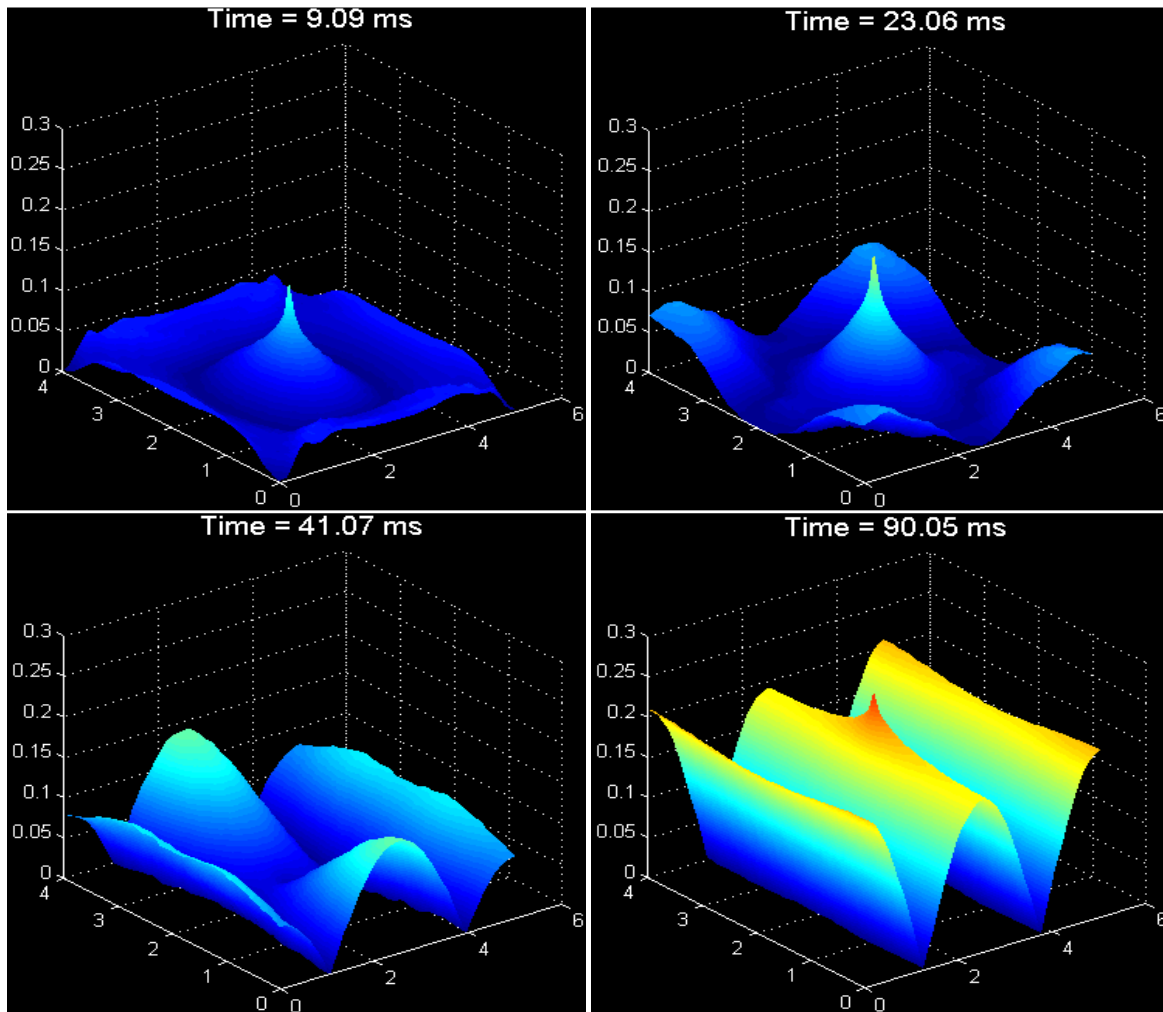


Figure 11: Steady state build-up of an axial mode at 68.6 Hz in a 2D 5 m x 4 m room

The toolbox can also handle the simulation of complex signals which can then be used to evaluate the performance effects of subwoofer placement and configuration. As such it is possible to compare for example, a single subwoofer with a multiple subwoofer system in terms of frequency response at various listening locations and to address the question, “*Does adding extra subwoofers help to reduce magnitude deviation and spatial variance within a room or do the extra subwoofers just increase these variations?*”

A simple simulation can be set up in a 5 m x 4 m x 3 m room with a 0.1 absorption coefficient on all walls. First, a single omnidirectional (i.e. point source) subwoofer is placed in the corner of the room and a 13th order Maximum Length Sequence (MLS) is played back while monitoring the response at 25 virtual listening points distributed throughout the room. From these measurements, each point's frequency response is calculated and compared to the others in the set, see Figure 12.

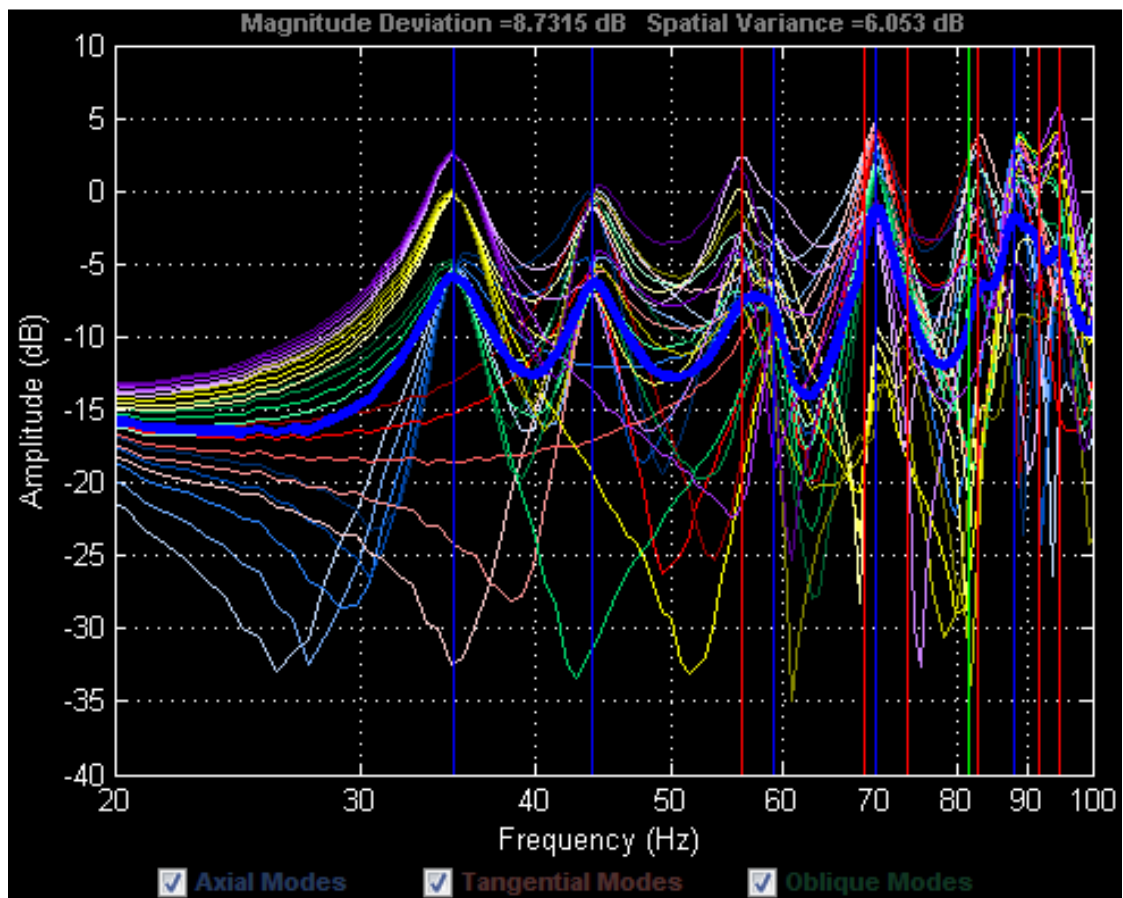


Figure 12: Simulated frequency response of 25 listening points in a 5 m x 4 m x 3 m room with a single subwoofer placed in the corner

While only examining over a frequency range from 20 Hz to 100 Hz (approximate range of a subwoofer), the listening locations' frequency responses tend to vary widely from one another, resulting in a spatial variance of over 6 dB. At certain points along the spectrum, points with shades of the same color (same listening row) seem to follow one another closely while at other points are very different. The large dips in response below the first axial mode around 35 Hz can be attributed to comb filtering due to the distance between the source, listening location and first reflection off the rear wall.

With these results in mind, a user can now explore the possibility of adding an extra subwoofer to improve the system response. At first, a second subwoofer will be added to the opposite corner of the room without any time delay or any other extra processing, see Figure 13.

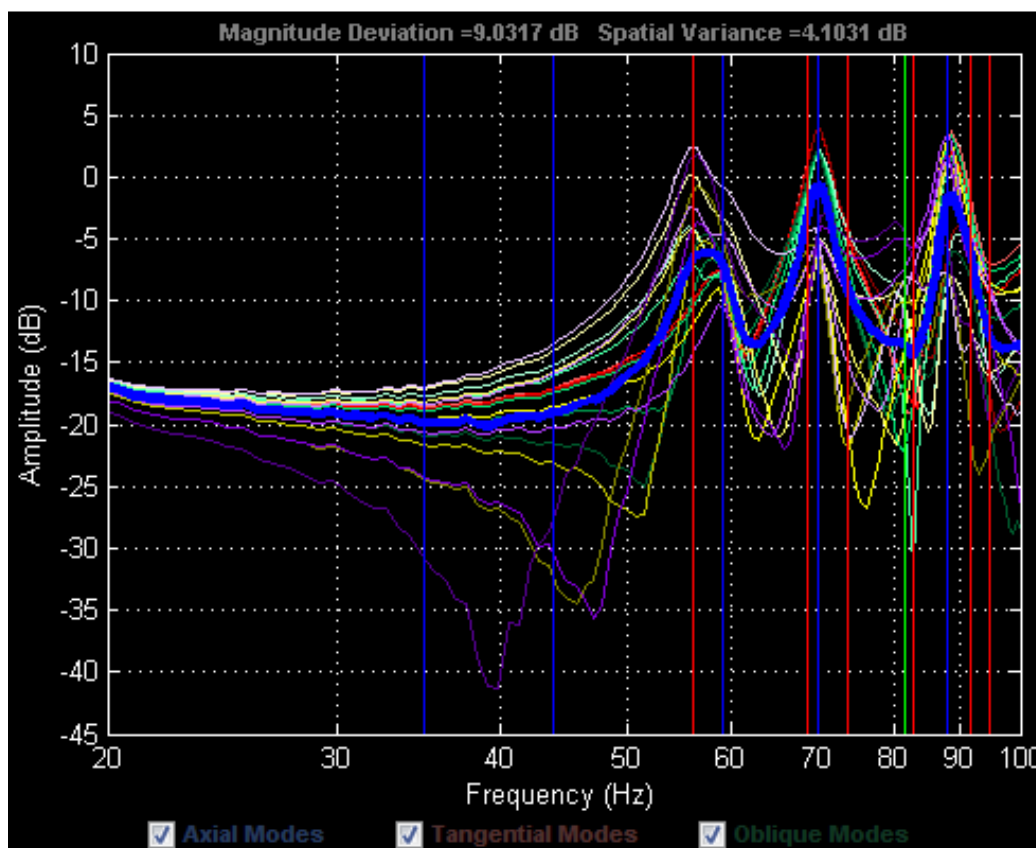


Figure 13: Simulated frequency response of 25 listening points in a 5 x 4 x 3 m room with two subwoofers placed at opposite corners

With an extra subwoofer added to the system, there is a clear improvement in the overall system response. The spatial variance has decreased to nearly 4 dB while the first two axial modes appear now not to affect the response because of destructive acoustical interference between the two subwoofers. This solution is not perfect since higher order modes are still equally present as in the single subwoofer system and while some comb filtering issues have been resolved, new ones have been introduced. Nevertheless, this system is an improvement over the single subwoofer system.

Next, the placement of the two subwoofers can be experimented with, for example moving them from the room corners to opposing wall midpoints. This move could help to further reduce the effect of room modes on the overall response again due to acoustical interference between the two subwoofers, see Figure 14.

Once again, the adjustment to the system has improved the overall response. With the subwoofers now placed at opposite wall midpoints, the first two axial and first tangential modes appear to have no effect on the response. Also, the unwanted comb filtering effects at very low frequencies have been almost entirely eliminated. The shift in subwoofer position has reduced the spatial variance to just less than 3 dB, which is less than half of the initial spatial variance with the single subwoofer system.

To conclude this exploration of subwoofer configurations, a second set of two subwoofers can be added to the system at the remaining two wall midpoints. Based on the pattern seen in the previous experiments, it would be anticipated that these additional subwoofers will realize an even better overall room response; this is confirmed by the results in Figure 15.

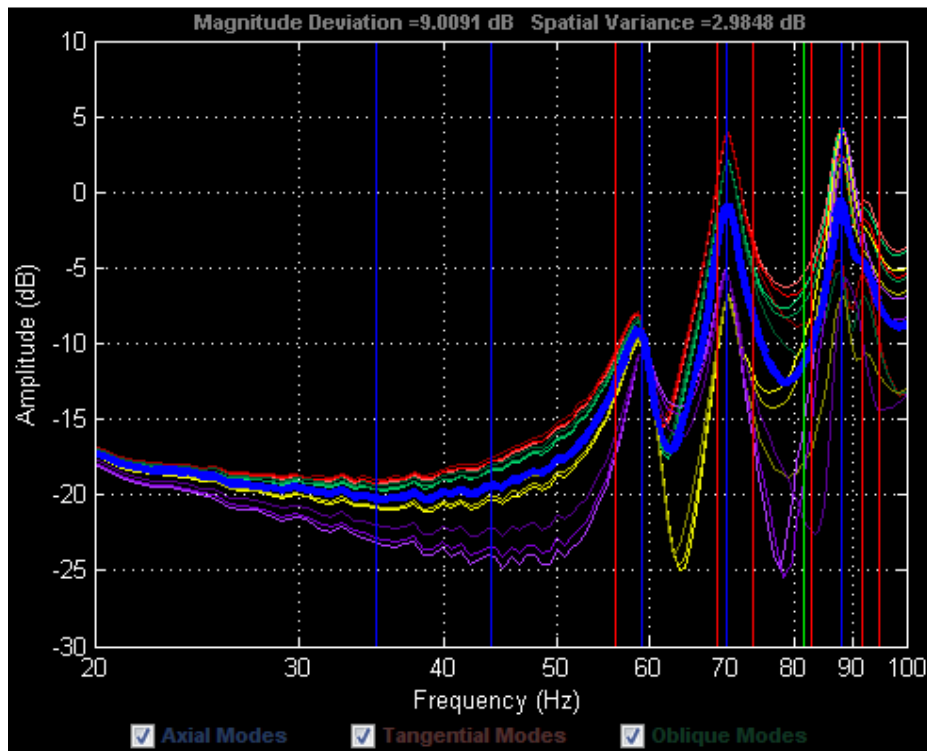


Figure 14: Simulated frequency response of 25 listening points in a 5 m x 4 m x 3 m room with two subwoofers placed at opposite wall midpoints

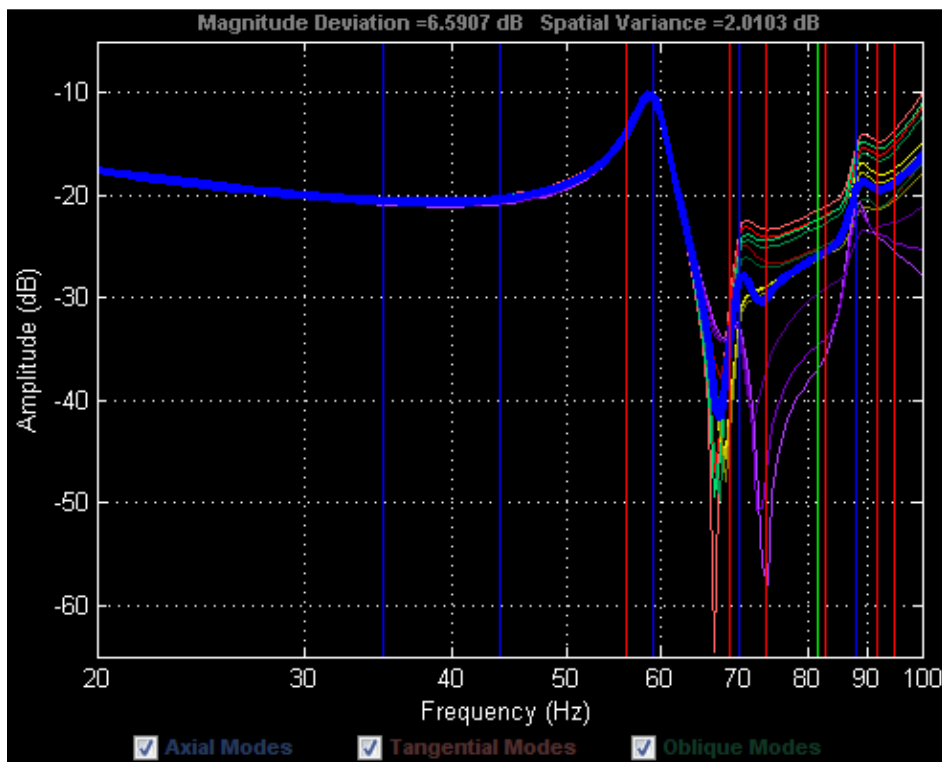


Figure 15: Simulated frequency response of 25 listening points in a 5 m x 4 m x 3 m room with four subwoofers placed at the wall midpoints

As expected, the four-subwoofer system is superior to the three previously discussed systems. All twenty-five listening points follow each other almost exactly up to around 70 Hz, which is reflected with a smaller spatial variance of around 2 dB. Since the frequency response of all points are now closely matched, global equalization could be applied to the entire system to help reduce the magnitude deviation, which otherwise would be similar to that of the single subwoofer system.

In addition to analyzing the loudspeaker-room interaction, the simulation toolbox can be used to explore in detail the diffraction of sound, where an example of this capability is a two-room system with a common open doorway as shown in Figures 16 and 17. These results can be compared to Olson's work¹³ for further validation.

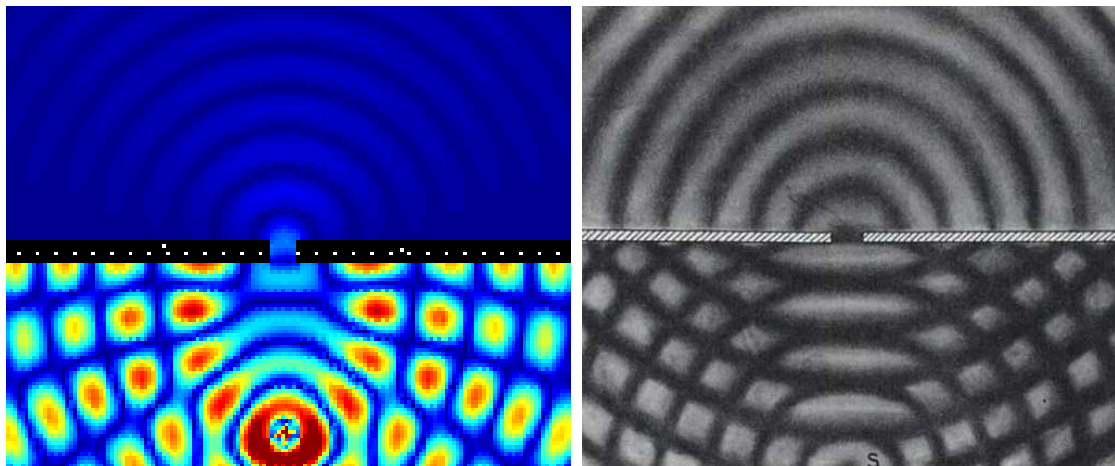


Figure 16: Sound diffraction example with a small opening in a reflecting wall (Simulation = left, Olson¹³ = right)

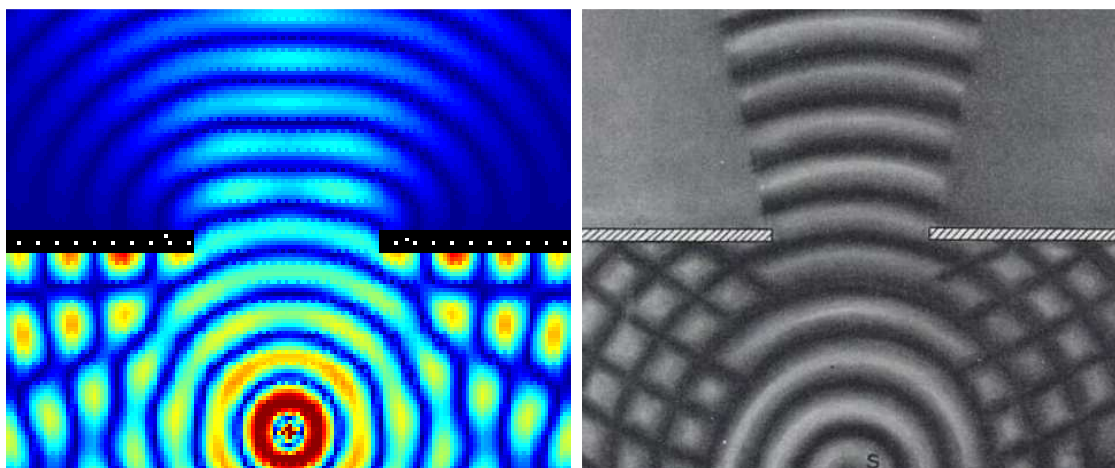


Figure 17: Sound diffraction example with a large opening in a reflecting wall (Simulation = left, Olson¹³ = right)

These examples help illustrate the difference between a large and small opening between rooms, where this could possibly be related to the difference between fully and partially open doorways. Clearly, there is a considerable difference between the two scenarios, especially for the room without the sound source. This example can be expanded to include a large network of differently shaped rooms to explore how a playback system in one room can affect other parts of an office or a house, see for example Figure 18. In addition, this technique could be used to explore the acoustics inside a vented loudspeaker enclosure using a Helmholtz resonator.

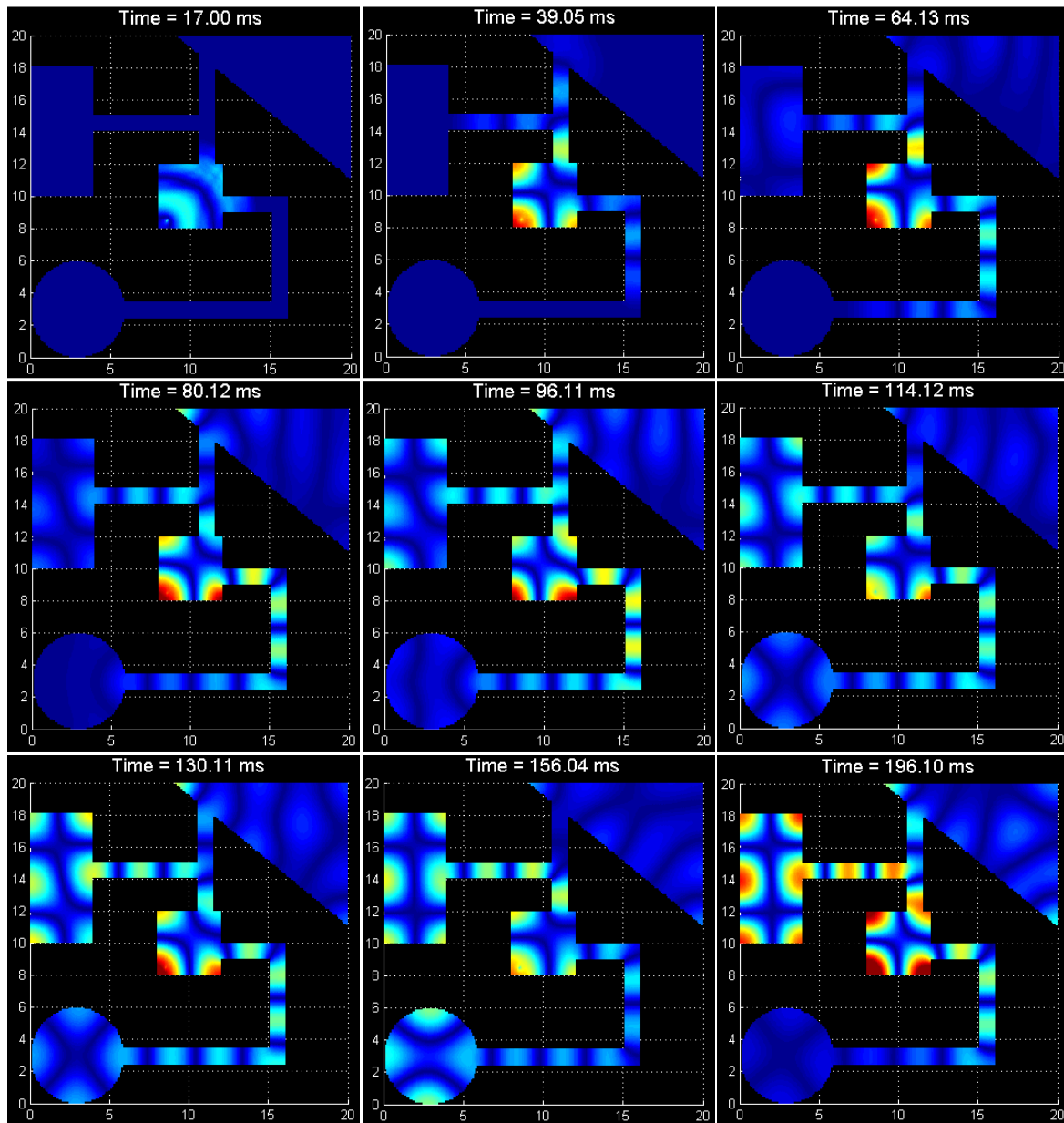


Figure 18: Simulated propagation of sound through a network of rooms laid out over a 20 m x 20 m space with a 60 Hz sinusoidal source located in the lower left corner of the central room

In addition to simulating the interaction of sound between adjacent rooms and hallways, the effect of obstacles within a room can also be explored with the toolbox, again comparing to the results of Olson¹³ (Figure 19). Finally, moving the simulation into the three-dimensional domain, it is possible to simulate common shapes of non-rectangular rooms having for example a domed ceiling, see Figure 20.

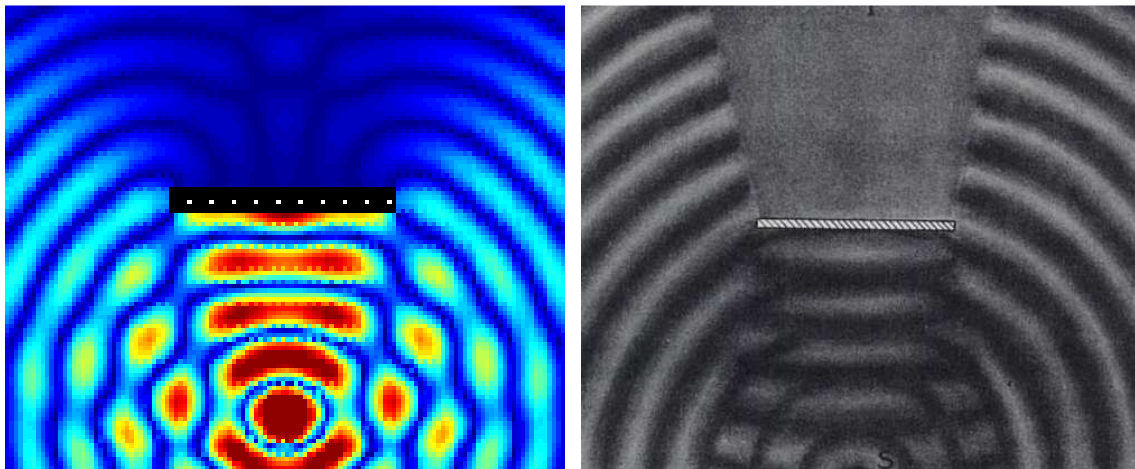


Figure 19: Sound diffraction example with a large obstacle in a room (Simulation = left, Olson¹³ = right)

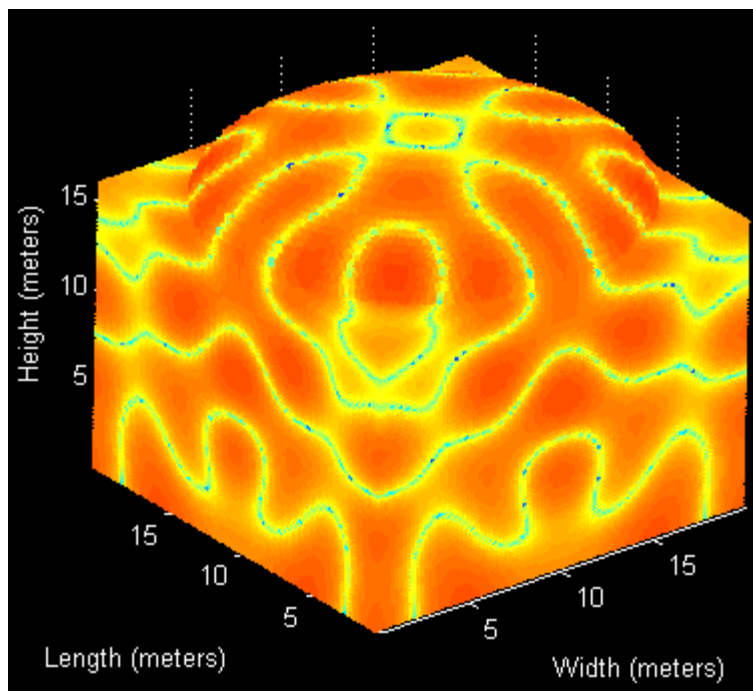


Figure 20: Simulation of a domed room with overall dimensions 20 m x 20 m x 20 m and a single source located on the center of the floor running at 60 Hz

6 CONCLUSION

The FDTD simulation toolbox described in this paper is a powerful tool for investigating a multitude of different acoustical scenarios. The inner structure of the program is rooted in a well-established simulation method (FDTD) which has been well-proven in electromagnetics and has been recently gaining great popularity in acoustics. To make the program as easy to use as possible, a simply laid out graphical user interface was written in Matlab which allows a user to access any function of the program from a single window.

The key attribute of this toolbox is the ability to visualize by rapid animation a sound wave's propagation through a room of any shape and size with the ability to monitor the response at a number of user-defined locations. A secondary yet powerful feature is the ability to auralize sound reproduced from within the virtual acoustic space in order to enable subjective evaluation of the interactions between rooms, loudspeakers and signal processing. Future work on the toolbox will allow for the analysis of various equalization techniques, primarily focusing on low-frequency control techniques. This will hopefully lead to a novel approach to adaptive low-frequency equalization in small to medium sized listening rooms without the need for excessive passive absorption or unrealistically complicated playback systems.

This software code was developed to assist in the current research of the authors and has not been intended for commercial use. The toolbox has been and will hopefully continue to aid in the ongoing research into low-frequency control in listening rooms.

7 REFERENCES

1. Salava, Tomas. "Subwoofers in small listening rooms." AES Convention #106, Preprint 4940. May, 1999.
2. Backman, Juha. "Low-frequency polar pattern control for improved in-room response." AES Convention #115, Preprint 5867. October, 2003.
3. Ferekidis, Lampos; Uwe Kempe. "The beneficial coupling of cardioid low frequency sources to the acoustic of small rooms." AES Convention #116, Preprint 6110. May, 2004.
4. Waterhouse, Richard V. "Output of a sound source in a reverberation chamber and other reflecting environments." Journal of the Acoustical Society of America. Volume 30 Issue 1, pp4-13. January, 1958.
5. Welti, Todd; Allan Devantier. "Low frequency optimization using multiple subwoofers." JAES Volume 54 Issue 5. May, 2006.
6. Celestinos, Adrian; Sofus Birkedal Nielson. "Optimizing placement and equalization of multiple low frequency loudspeakers in rooms." AES Convention #119, Preprint 6545. October, 2005.
7. Welti, Todd. "How many subwoofers are enough?" AES Convention #112. Preprint 5602. May, 2002.
8. Toole, Floyd E. *Sound Reproduction: Loudspeakers and Rooms*. Focal Press, New York, 2008.
9. Schroeder, M.R. "Statistical parameters of the frequency response curves of large rooms." *Acustica*. Volume 4, pp594-600. 1954.
10. Schroeder, M.R. "'Schroeder Frequency' revisited." Journal of the Acoustical Society of America. Volume 99 Issue 5, pp3240-3241.
11. Hill, Adam J; Malcolm O.J. Hawksford. "Visualization and analysis tools for low frequency propagation in a generalized 3D acoustic space." AES Convention #127, Preprint 7901. October, 2009.
12. Olesen, Soren Krarup. "Low frequency room simulation using finite difference equations." AES Convention #102, Preprint 4422. March 1997.
13. Olson, Harry F. *Music, Physics and Engineering*. Dover Publications, Inc. New York. 1967.